X-Ray photoelectron spectroscopy characterization of amorphous and crystalline poly(tetrahydrofuran): experimental and theoretical study

P. Boulanger*, J. J. Pireaux†, J. J. Verbist and J. Delhalle‡
Laboratoire Interdisciplinaire de Spectroscopie Electronique, and ‡ Laboratoire de Chimie Théorique Appliquée, Facultés Universitaires Notre-Dame de la Paix, 61 rue de Bruxelles, B 5000 Namur, Belgium
(Received 14 March 1994)

Measurements of the X-ray photoelectron spectroscopy (Xp.s.) valence-band spectra of crystalline and amorphous poly(tetrahydrofuran) are reported. The experimental data are analysed on the basis of theoretically simulated Xp.s. valence-band spectra of model molecules. Differences in the spectra of poly(tetrahydrofuran) in amorphous and crystalline phases are interpreted in terms of differences in the conformational characteristics of the macromolecular chains.

(Keywords: poly(tetrahydrofuran); characterization; photoelectron spectroscopy)

INTRODUCTION

Owing to the increasing need for detailed characterization of the interfacial structure in multicomponent materials, techniques such as X-ray photoelectron spectroscopy (Xp.s.) and u.v. photoelectron spectroscopy (u.v.p.s.) are today routinely used in academic and industrial laboratories. Their sampling depth (1–10 nm) makes Xp.s. and u.v.p.s. genuine surface analysis techniques to obtain information on the first molecular layers at the surface of solids (such as polymer, semiconductor, ceramic, glass, metal, alloy).

In the polymer field, Xp.s. is used mainly to characterize the elemental and chemical compositions and primary structure of polymer chains from the core-line positions, shifts and intensities. In a limited number of materials, such as poly(tetramethyl-*p*-silphenyl-siloxane)[1] or alcane–styrene copolymer[2], information on the secondary structure of the polymer chains in the topmost layers has been gained through a quantitative analysis of the spectral features of the core-level peaks. These remain exceptions because the high electron binding energy region is rather insensitive to conformational changes. However, as shown by quantum mechanical calculations[3], the valence-band part of Xp.s. spectra, typically ranging from 0 to 40 eV, conceals information on the primary and secondary structure of the polymer chains. The emphasis of such studies so far has been on pure hydrocarbon oligomers and polymers[4–12], but a limited number of studies along these lines have also been reported in recent years on oxygen-containing polymers such as poly(oxymethylene)[13,14], poly(ethylene oxide)[15,16], poly(vinyl alcohol)[15] and poly(ethylene terephthalate) (PET)[17].

In the case of poly(oxymethylene), the measured Xp.s. valence spectra[14] have been found to be in good qualitative agreement with theoretical predictions. Furthermore, the highly crystalline orthorhombic and hexagonal forms, of which chains differ only by one of their torsional angles, present definite differences that have been interpreted in terms of conformational effects. Even if work on the structurally best defined and well characterized polymer surfaces should intensify in the future, to determine the conditions and limits for such studies, it is also worthwhile to investigate more realistic systems. It is in this spirit that we have recently studied the Xp.s. valence-band spectra of amorphous and crystalline (48%) PET[17]. At the limit of the Xp.s. technique sensitivity, it has been possible to ascribe the origin of the observed differences to geometrical effects in the glycolic moieties of PET chains, which mostly adopt either a *gauche* or a *trans* conformation in the amorphous and crystalline phases, respectively.

The present contribution provides another example of the use of the Xp.s. valence spectra to characterize polymer surfaces. Here, we compare experimental Xp.s. valence-band spectra of poly(tetrahydrofuran) (PTHF) in very different morphologies, i.e. amorphous (completely disordered) *versus* crystalline (ordered) phases. The interpretation of the experimental data is carried out on the basis of simulated Xp.s. valence-band spectra calculated on molecules modelling the PTHF polymer chains.

MODEL XP.S. VALENCE SPECTRA OF PTHF CHAINS

Model systems

PTHF is a soft linear polyether with $-CH_2-CH_2-CH_2-CH_2-O-$ as the monomeric unit. The amorphous polymer

* Permanent address: Glaverbel SA, Centre de Recherches et Développement, 2 rue de l'Aurore, B-6040 Jumet, Belgium
† To whom correspondence should be addressed

0032-3861/94/24/5185–09

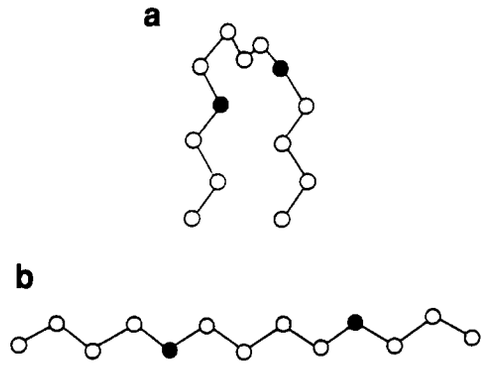

Figure 1 Representation of (a) 1,4-butanediol propyl butyl ether (BDPBE) molecule with a folded conformation and (b) 1,4-butanediol dibutyl ether (BDDBE) molecule with planar zigzag conformation

can be crystallized by annealing[18] for 1 h at 0°C as confirmed by i.r. spectroscopy measurements (see Experimental section). In this ordered state, PTHF macromolecules take a fully planar zigzag (or *trans*) molecular conformation and form crystals with monoclinic unit cells[19,20], each containing two polymer chains. Owing to computing limitations, the chosen model molecules are 1,4-butanediol dibutyl ether (BDDBE) or CH_3–$(CH_2)_3$–O–$(CH_2)_4$–O–$(CH_2)_3$–CH_3, and 1,4-butanediol propyl butyl ether (BDPBE) or CH_3–$(CH_2)_2$–O–$(CH_2)_4$–O–$(CH_2)_3$–CH_3, both containing two oxygen atoms. We have shown in previous studies[3–17] that molecules of this size are usually sufficient to provide reliable simulations of Xp.s. valence spectra of saturated systems.

Input geometrical parameters are as follows: bond distances, d, 1.54 Å (d_{C-C}), 1.43 Å (d_{C-O}) and 1.09 Å (d_{C-H}), and all valence angles assumed to be tetrahedral. Since we are aiming at a qualitative description of the spectra, this assumption of the valence angles is reasonable because the C–O–C angle in related systems is indeed close to the tetrahedral value. For instance, this angle is equal to 111.7° and 109.9° in dimethyl ether[21] and in poly(oxymethylene)[22], respectively. The molecule modelling PTHF chains in the crystalline state is in a fully planar zigzag conformation, i.e. all torsional angles equal to 180°, as shown in *Figure 1*. Molecular conformations in the amorphous state are randomly distributed along the chain so that rigorous modelling of an actual disordered molecule is impossible. However, if we consider that a molecule in the amorphous state contains many folds, it is reasonable to use a small folded molecule to model the PTHF polymer chains in the non-crystalline regions. The molecular parameters used to describe the molecular fold are those determined by Petraccone *et al.*[23] for the optimized folded hexatriacontane molecule ($C_{13}H_{28}$) (see *Figure 1*). To comply with this fold, the molecule used to model amorphous PTHF is BDPBE, which contains two butyl and one propyl group (13 atoms) in place of three butyl segments (14 atoms) in the planar zigzag model molecule. The incidence on the simulated Xp.s. valence-band spectra will be discussed later.

Calculations

All the calculations reported in this work have been carried out at the *ab initio* level using the Gaussian 82 program[24]. Owing to the size and the low symmetry of the model molecules, on the one hand, and the need to use the Gelius intensity model[25] to obtain simulations of the Xp.s. valence spectra, on the other hand, we have chosen to use the minimal STO-3G basis set. The requested convergence on density matrix was fixed at 10^{-8} and the integral cut-off was fixed at 10^{-8} hartree. Although this calculation method is simple, we are confident in the qualitative ordering of one-electron states, as already proved by similar work on the chemically related poly(oxymethylene) and poly(ethylene oxide)[13–16].

According to Koopmans' theorem[26], the theoretical ionization potentials can be approximated by the negative value, $-\varepsilon_i$, of the calculated one-electron energy levels. Theoretical Xp.s. peaks are then represented by a 50/50 linear combination of Lorentzian and Gaussian curves (full-width at half maximum, $FWHM = 1.5$ eV) centred on the one-electron state energy value, ε_i. The peak heights are calculated according to the Gelius model[25]. Since the contributions of the 1s atomic orbitals are not significant in the valence molecular states, they are not accounted for. The relative atomic photoionization cross-sections used for C2s, C2p, O2s, O2p, H1s are 1.000, 0.077, 1.400, 0.159 and 0.0, respectively. A theoretically simulated Xp.s. valence-band spectrum is obtained by summing the contributions from all the one-electron molecular states.

When comparing experimental and simulated experimental spectra, the simplicity of the model must be kept in mind. First, experimental valence-band structures are broadened by solid-state effects originating mainly from vibrational excitations in the ionized state, which are not included in the model. Second, in the frozen orbital approximation chosen here, intra- and intermolecular electronic relaxations are neglected. They contribute to the stabilization of the ionized molecule and consequently lead to lower binding energies. This is due to the redistribution of the positive charge on the ionized system (intramolecular process) and by long-range polar interactions (intermolecular process). It is reasonable to think that the intramolecular relaxation (polarization) energies for the valence (and core) levels in amorphous and crystalline PTHF are the same, but intermolecular relaxation energies could be different. Indeed, Sato *et al.*[27] have shown that the polarization energy, P, can be related to the molecular volume, v, according to the relation:

$$P = K\left(\frac{e}{4\pi\varepsilon_0}\right)^2 \frac{\alpha}{2v^{4/3}}$$

where e is the electron charge, α is the molecular polarizability, ε_0 is the solid dielectric constant and K is a constant. So, the intermolecular relaxation energy should be larger for a more compact crystalline solid than for an amorphous one, as has been confirmed for some molecular solids. For example, the polarization energy difference between amorphous and crystalline pentacene has been measured as 0.3 eV by Seki *et al.*[28].

In this type of qualitative work[2–17], comparison with experimental data is often facilitated by contracting and shifting the theoretical binding-energy scale according to the empirical relation:

$$\varepsilon'_i = 0.82\varepsilon_i - 2.90$$

obtained from the linear regression correlating the corresponding experimental and theoretical peak positions.

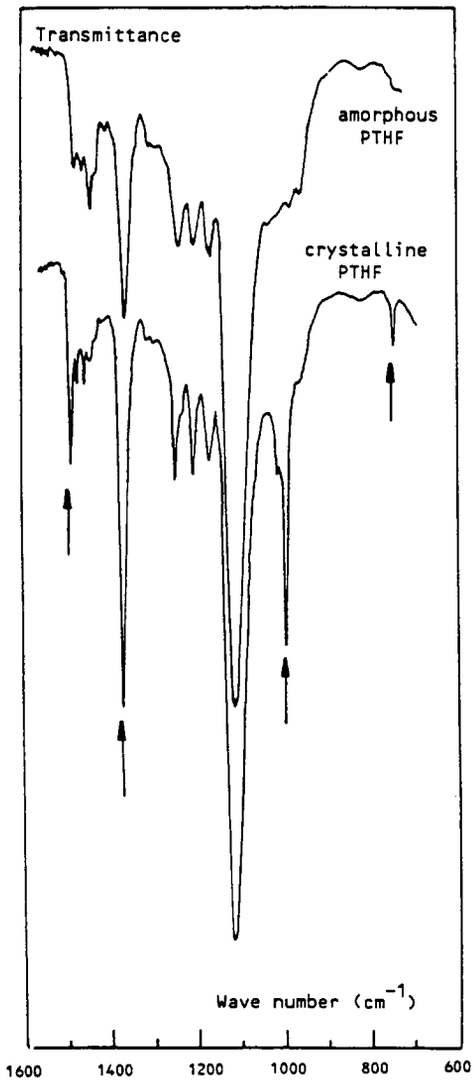

Figure 2 I.r. spectra of PTHF in amorphous and crystalline phases (arrows indicate crystalline bands). See *Table 1* for the assignment of the bands

EXPERIMENTAL

Preparation of the samples

The PTHF polymer was supplied by Polysciences (cat. no. 8292) and had a molecular weight of ~130 000 and a melting point of 45°C. An amorphous PTHF film (~1 μm thick) was obtained by solvent casting of a 0.1% PTHF solution in chloroform. The film was deposited onto a suitable substrate: NaCl crystal or polished stainless steel plate for i.r. or Xp.s. measurements, respectively. The annealing treatment of the film that enables PTHF to crystallize at 0°C was maintained for 1 h, according to the procedure recommended by Kretz *et al.*[18].

Transmission i.r. spectra were recorded on a Perkin–Elmer 850 apparatus.

Xp.s. measurements

Photoelectron spectra were recorded with a Hewlett-Packard 5950A spectrometer using Al Kα monochromatized radiation ($h\nu = 1486.6$ eV). Polymer samples were introduced into a vacuum chamber (pressure $< 10^{-8}$ torr; 1 torr = 133.3 Pa). Owing to the insulating nature of PTHF, the positive charge at the sample surface during analysis was stabilized by using an electron flood gun with low energy ($E < 4$ eV) and current ($I < 1$ mA). Moreover, analysed samples were cooled to 263 K during the analysis in order to prevent their degradation under the X-ray beam. Possible modifications at the surface were controlled by regularly checking the C1s and O1s core-level spectra. Owing to the low signal-to-noise ratio in the valence-band energy region, a typical valence-band spectrum was obtained by summing several recordings, each one accumulated for 6 h.

Calibration of the spectra was obtained by referencing to the binding energy of the C1s levels, themselves calibrated by mixing the polymer with poly(trifluoroethylene) (C̲HF– and C̲F$_2$– core-level peaks localized at 289.4 eV and 291.6 eV, respectively)[4].

RESULTS AND DISCUSSION

I.r. spectroscopy measurements

The i.r. spectra of amorphous and crystallized PTHF films presented in *Figure 2* show significant differences, which are summarized in *Table 1*. According to previous studies[29,30], these differences are interpreted as originating from structural modifications in the polymeric chains in both phases. So, i.r. bands located at 1490, 1372, 996 and 746 cm^{-1} are attributed to normal modes of PTHF macromolecules in the crystalline phase. In addition, the peak at 745 cm^{-1} is considered to be a spectroscopic signature of a planar zigzag conformation as adopted by the polymer chains in the crystalline phase. This observation is verified for many polymers such as polyethers, polythioethers and polyesters[31]. Therefore, we can be confident, on this i.r. basis, that the PTHF films submitted to the Xp.s. analysis are indeed in the amorphous and crystalline morphological states, as described in the literature. One word of caution, however, is in order: i.r. spectroscopy results are concerned with a material thickness of about 1 μm, while Xp.s. samples only the topmost layers, up to ~10 nm.

Xp.s. results

Core-level spectra. Core-level spectra of the PTHF polymers in amorphous and crystalline phases are presented in *Figure 3*. In order to clarify the discussion, the carbon atoms of the ether function in the monomer unit are labelled C_a, and the hydrocarbon-type carbon atoms are labelled C_b as follows: –O–[C_aH_2]–[C_bH_2]–CH_2–CH_2–. *Table 2* summarizes the spectral data, namely: binding energies of the different core-level peaks; total carbon (C_t) *versus* oxygen (O) atomic contents; ether carbon (C̲$_a$–O) *versus* hydrocarbon-type carbon (C̲$_b$)

Table 1 Frequency and assignment of the i.r. crystalline absorption bands in amorphous and crystallized PTHF, –(CH_2–[CH_2]$_{II}$–[CH_2]$_I$–CH_2–O)–

Frequency (cm^{-1})	Intensity		Assignment
	Crystalline	Amorphous	
1490	Large	Absent	$\delta(CH_2)_I$–$\delta(CH_2)_{II}$ + w$(CH_2)_I$
1372	Large	Medium	w$(CH_2)_I$–ν_a(COC)
996	Large	Weak	ν_s(COC)–ν_a(CC)
746	Large	Absent	r$(CH_2)_I$ + r$(CH_2)_{II}$

δ, Bending; w, wagging; ν_a, antisymmetric stretching; ν_s, symmetric stretching; r, rocking

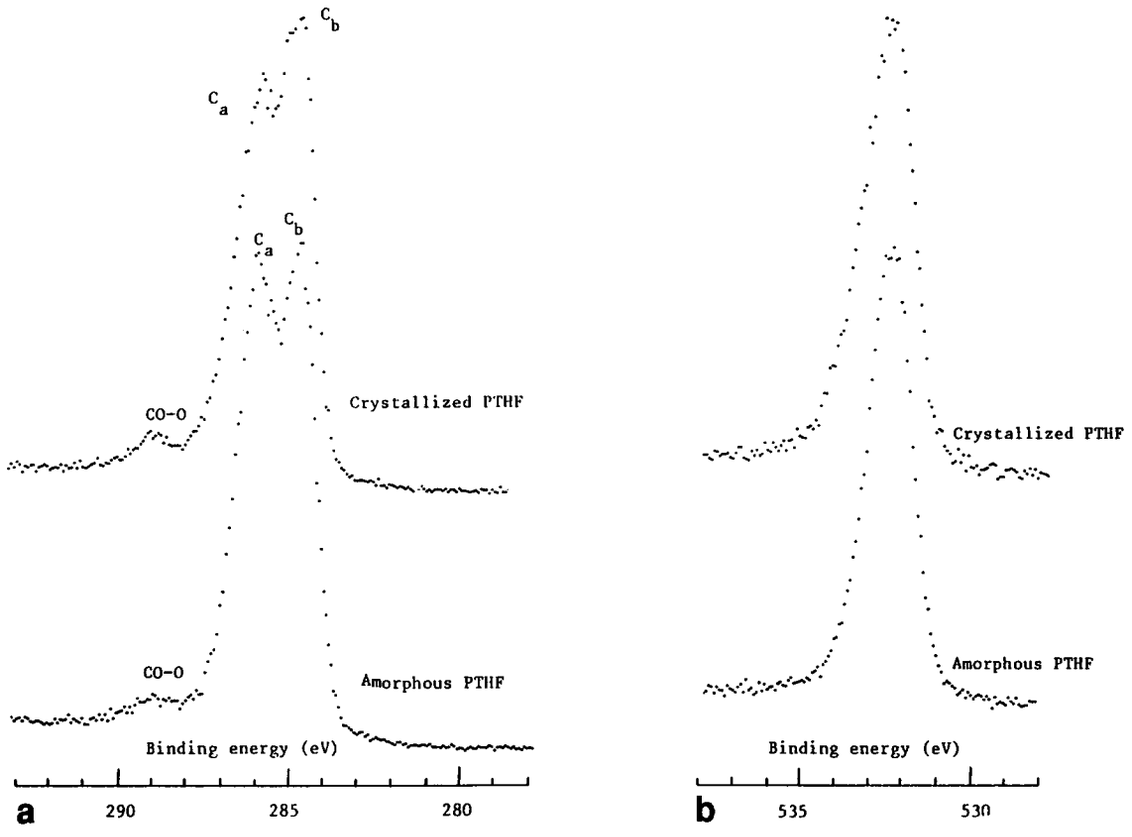

Figure 3 Carbon 1s (a) and oxygen 1s (b) Xp.s. core-level spectra of PTHF in crystalline and amorphous states

Table 2 Binding energies, total carbon (C_t) *versus* oxygen atomic contents, ether carbon ($\underline{C}_a$–O) *versus* hydrocarbon-type carbon ($\underline{C}_b$) ratios and carboxylic carbon ($\underline{C}$O–O) *versus* total carbon atomic contents in the core-level spectra of PTHF polymers in amorphous and crystalline phases

PTHF morphology	Binding energy (eV)				$\frac{\underline{C}_a\text{–O}}{\underline{C}_b}$		$\frac{C_t}{O}$		$\frac{\underline{C}O\text{–O}}{C_t}$
	$\underline{C}_a$–O	$\underline{C}_b$	$\underline{C}$O–O	O–$\underline{C}$	Expt	Theory	Expt	Theory	
Crystalline	286.1	284.8	289.1	532.4	0.94	1.0	4.20	4.00	0.03
Amorphous	286.1	284.8	289.1	532.4	0.96	1.0	3.88	4.00	0.01

ratios; and the carboxylic ($\underline{C}$O–O) *versus* total carbon atomic contents.

The C1s core-level spectra of PTHF in both phases contain three peaks: the two intense ones correspond, as expected, to ether carbon (O–$\underline{C}_aH_2$) and to hydrocarbon-type carbon ($\underline{C}_bH_2$), respectively. However, in both spectra, a small structure appears at a binding energy of 289.0 eV and is attributed to carboxylic $\underline{C}$O–O functions, probably resulting from polymer synthesis. As this peak represents only 1–3% of the total carbon intensity, the valence-band spectrum should not be dramatically perturbed and should reproduce the electronic structure of the pure polymer. More surprising is the discrepancy between the total carbon *versus* oxygen atomic contents: 4.20 and 3.88 in the crystalline and amorphous phases, respectively. According to experimental $\underline{C}_a$–O/$\underline{C}_b$ ratios, it is seen that the content in the hydrocarbon-type carbon is larger in the crystalline than in the amorphous PTHF. The origin of this difference could be attributed to surface contamination during crystallization of the polymer. However, it is worth noting here that an enrichment of the surface layers in $\underline{C}_bH_2$ methylene groups, due to a particular conformational arrangement of molecular chains, is not to be ruled out. Unfortunately, it is not possible to ascertain this fact at this stage.

Valence-level spectra. Before discussing geometrical effects in the polymer chains on the shape of the Xp.s. valence band, it is worthwhile to understand the origin of the Xp.s. valence peaks in the PTHF spectra. Therefore this section deals first with the interpretation of the main structures in Xp.s. spectra of crystalline PTHF on the basis of theoretical calculations, and second, compares the simulated and measured Xp.s. valence-band spectra of PTHF in both crystalline and amorphous phases.

(a) *Bonding nature of the levels in the valence band of crystalline PTHF.* Simulated and experimental spectra of crystalline PTHF polymer (planar zigzag form) are shown in *Figure 4* and positions on the binding-energy scale of the main peaks are summarized in *Table 3*. As previously mentioned in similar studies on oxygenated polymers[13–17], four distinct regions, called A, B, C and D, are clearly identified in the Xp.s. valence-band spectra. They are the fingerprints of molecular levels

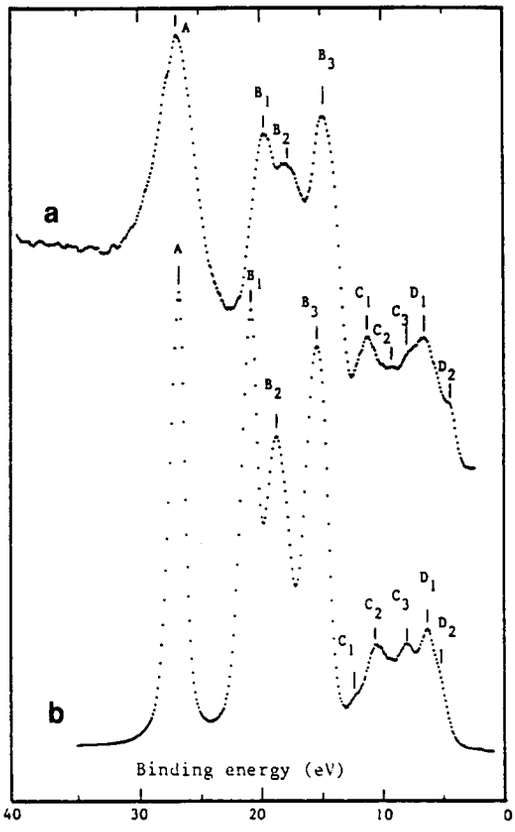

Figure 4 (a) Experimental Xp.s. valence-band spectrum of PTHF in crystalline phase and (b) simulated Xp.s. valence-band spectrum of BDDBE molecule with planar zigzag conformation

where the main atomic orbital participations are: O2s (A), C2s–O2s (B), C2p–O2p–H1s (C) and O2p (D). Good overall agreement between simulated and measured spectra is found.

Region A. This region contains one peak located at 26.3 eV (26.07 eV in simulated spectra). This structure issues from molecular levels originating from bonding interactions between adjacent oxygen and carbon atoms forming the σ_{COC} (2s) ether bond. The presence of an intense structure at about 26 eV is thus a signature of an ether function in the monomeric unit, as discussed previously for other polyethers such as poly(ethylene oxide)[15,16]. There is a marked difference in the *FWHM* of peak A in the experimental ($FWHM = 3.5$ eV) and theoretical ($FWHM = 1.5$ eV) spectra. The origin of this difference is beyond the scope of this work; it could be due to bulk effects, but correlation effects[32], not accounted for within the level of theory used in this work, cannot be ruled out.

Region B. In both simulated and measured spectra, three structures (B_1, B_2 and B_3) can be seen: their predicted intensities and positions on the binding-energy scale are in good agreement with the measured ones. In order to understand the origin of these peaks, a simple scheme representing the main character of the molecular orbitals in this energy region for the BDDBE model molecule is shown in *Figure 5*. The three deeper energy levels represent mainly σ_{CC} bonding interactions in tetramethylene segments; they give rise to the B_1 peaks at 19.4 eV (20.19 eV in simulated spectra). The second B_2 structure, calculated at 17.38 eV, is due to molecular orbitals with a mixed σ_{CC} bonding and σ_{CO} antibonding character, as shown in *Figure 5*; the corresponding experimental structure is located at 17.2 eV. Finally, antibonding interactions between carbon in tetramethylene groups, σ_{CC}, and a smaller contribution in ether functions, σ_{CO}, are located around a binding energy of 14.8 eV and give rise to the simulated (and experimental) peak B_3.

Region C. This binding energy region originates from molecular levels with mixed C2p, O2p and H1s atomic characters. However, owing to the dispersion of the molecular levels (theory) and the low signal-to-noise ratio (experiment), a simple interpretation of these peaks is not straightforward. We therefore limit our account to a simple comparison between the shapes of the simulated and experimental Xp.s. valence band in region C. They are generally in good qualitative agreement, except for a shift toward high binding-energy values for the simulated C_3 peak.

Region D. Generally speaking, the characterization of the highest molecular levels, which determine the chemical reactivity in molecules and of course polymers, is important. In the case of PTHF model molecules and polymers, these levels are located in the binding-energy range of 7–0 eV, called region D. In both simulated and experimental spectra, two peaks, D_1 and D_2, are distinguished and their predicted positions (D_1 5.63 eV, D_2 4.51 eV) follow the measured data (D_1 6.3 eV, D_2 4.0 eV). Theoretical results on the BDDBE molecule allow a simple interpretation of these spectral structures. In this molecule, the highest occupied molecular orbital (HOMO) and HOMO-1 with dominant O2p atomic character ($\sim 80\%$) are almost degenerate; together they give rise to the D_2 band. Accordingly, the corresponding peak in the experimental spectrum, at 4.0 eV, is assigned to the lone electron pairs centred on the oxygen atoms in the polymer chains.

The HOMO-3 and HOMO-4 levels in the electronic structure of the model molecule represent bonding interactions between $C2p_x$, $O2p_x$ and O2s atomic orbitals, giving rise to σ_{COC} links. These levels generate structure D_1 at 5.63 eV. The high intensity is obviously due to the large ($\sim 14\%$) O2s atomic contribution. This prediction also fits the experimental data, as the D_1 peak appears at 6.1 eV in the measured spectrum.

Table 3 Positions on the binding energy scale (eV) and relative intensities (in parentheses) of peaks in simulated and experimental Xp.s. valence-band spectra of crystalline PTHF

	Theory		
Peak label	Contracted[a]	*Ab initio*	Experiment
A	26.07 (1.00)[b]	35.24	26.3[c] (1.00)
B_1	20.19 (0.93)	28.09	19.4 (0.83)
B_2	17.38 (0.63)	24.67	17.2 (0.77)
B_3	14.81 (0.79)	21.54	14.1 (0.98)
C_1	11.43	17.43	10.8
C_2	9.66	15.28	8.8
C_3	7.24	12.34	7.4
D_1	5.63	10.38	6.1
D_2	4.51	9.01	4.0

[a] *Ab initio* binding energies are contracted according to the empirical relation: $E_{contr.} = 0.82\ E_{ab\ initio} - 2.90$
[b] The intensities are normalized with respect to the A peak intensity
[c] Peak binding energy values are determined by using the second derivative procedure

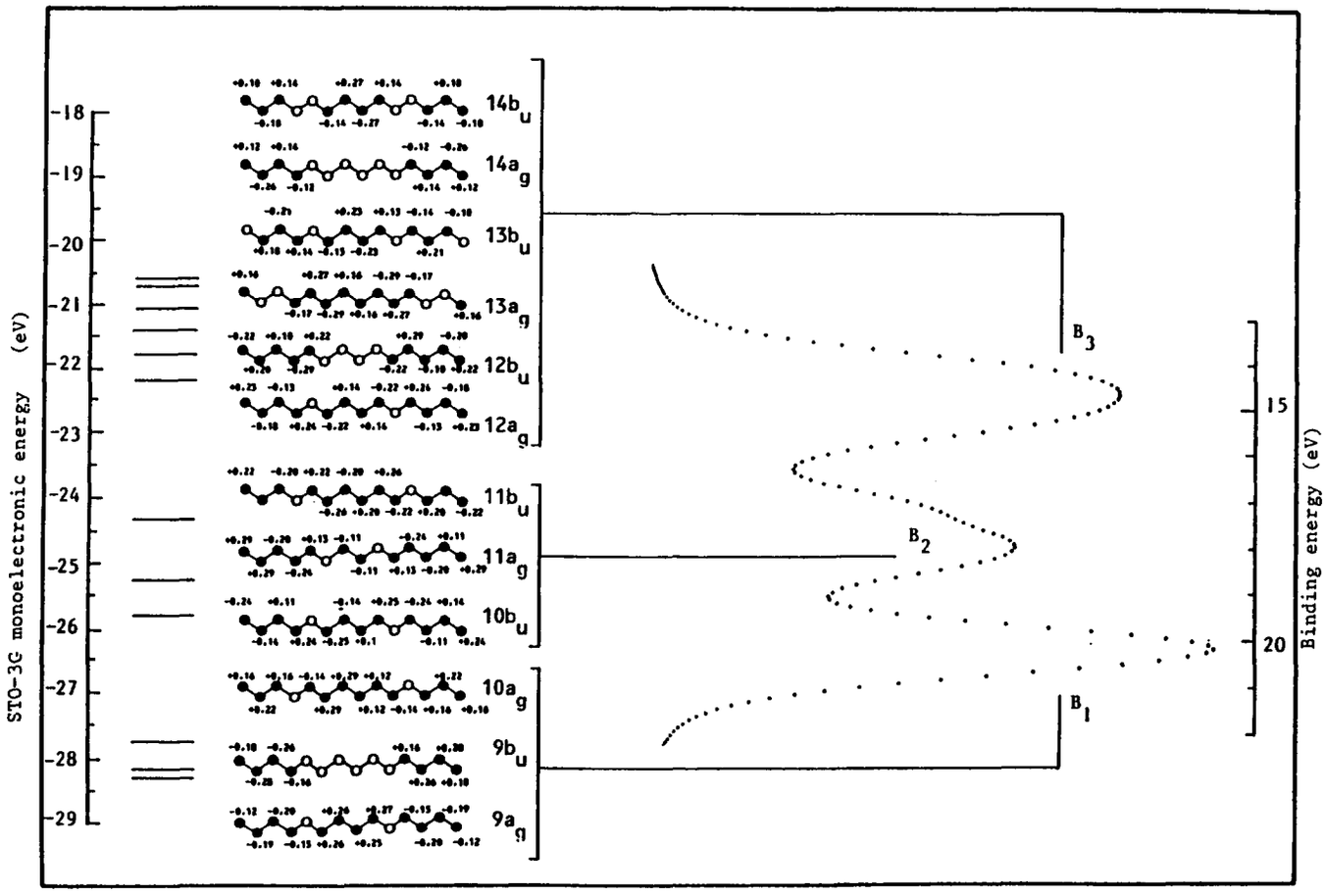

Figure 5 Schematic representation of the molecular levels giving rise to region B in the simulated valence-band spectrum of BDDBE molecule with planar zigzag conformation

(b) *Influence of the physical state of PTHF samples on the Xp.s. valence spectra.* As mentioned previously, the chain molecular structure in amorphous PTHF is modelled by BDPBE derived from a model of folded hexatriacontane, $C_{13}H_{28}$. In order to facilitate the study of the conformational effect, we will also compare simulated valence-band spectra of this molecule in planar zigzag and folded conformation.

Since BDDBE and BDPBE in different conformations will eventually be compared, we first analyse the changes in the simulated Xp.s. valence spectra of BDDBE and BDBPE simulated spectra (*Figures 6b* and *c*), both in the planar zigzag conformation. The main difference lies in region B, where the middle B_2 structure is lowered in intensity and broadened owing to the replacement of a butyl by a propyl segment.

If we now compare simulated spectra of BDBPE having folded and planar zigzag conformations (*Figures 6a* and *b*), some obvious differences are observed. First, structure B_3, appearing as a shoulder of B_2 in the spectrum of the planar zigzag form, disappears under folding. The most significant difference lies in region B, where the normalized intensity of B_5 structure is substantially lowered in the spectrum of the folded molecule. In addition, region C presents some small differences such as shifts in binding energy of structure (C_1) and changes of relative intensities (C_2 peaks).

We shall limit our analysis to the most evident feature, the relative intensity of structure B_5. On the basis of the theoretical results, a schematic representation of the molecular levels in this energy region is shown in *Figure 7*. It is seen that a fold in the molecule makes level 26 less stable compared to the corresponding level (26a') in the planar zigzag molecule. This is due to a difference in the participation of the C2p$_i$ (i=x, y and z) atomic orbital in the folded form compared to the planar zigzag form. As a consequence, the simulated Xp.s. B_5 peak will be broadened and lowered in intensity for the folded form. This is similar to the effect reported in the case of folds at the surface of polyethylene lamellae[8] and recently interpreted in terms of changes in hyperconjugation interactions along the polymer backbone when the chain conformation departs from the planar zigzag form[10].

Comparing experimental valence-band spectra of PTHF chains in the crystalline and amorphous states (*Table 4* and *Figure 8*) reveals that the following differences are also present. (i) As predicted by our theoretical models, the normalized intensity of peak B_5 is lower in the spectrum of molecules in the amorphous state. This observation supports the validity of a folded molecule to model polymeric chains in non-crystalline regions. (ii) The shape of region D in both spectra is different: for the crystalline polymer, structures D_1 and D_2 are located at lower binding energies (6.1 and 4.0 eV, respectively) while they appear at 6.5 and 4.3 eV for the amorphous polymer. In addition, an experimental C_3 peak appears as a shoulder of structure D_1 in the spectrum of the chains in the crystalline phase; this is not explained by our theoretical model.

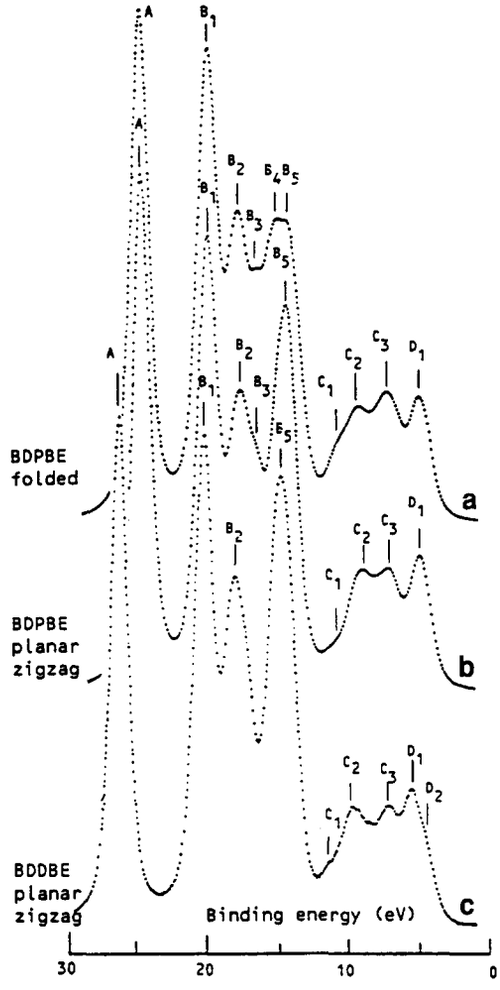

Figure 6 Simulated Xp.s. valence-band spectra of BDPBE molecule with (a) folded and (b) planar zigzag conformation and (c) BDDBE with planar zigzag conformation

As the observed differences in spectral D regions are not revealed in the theoretical spectra presented in *Figure 6*, we suggest two explanations. First, we can suppose that calculations performed on a simple folded molecule containing 14 atoms are only able to account for the most important modifications in the electronic structure of region B (from 20 to 13 eV on the binding-energy scale). Reliable prediction of such conformational effects in external electronic levels (region D) would probably require calculations on larger molecules having some randomly distributed folds. Second, it is reasonable to stress a difference in polarization energy between the amorphous and crystalline states to explain the relative destabilization of D peaks in the crystalline polymer. Indeed, a shift toward lower binding-energy values is observed for most of the peaks in the spectrum of crystallized PTHF (see *Table 4*). As previous measurements on molecular solids[28] have clearly demonstrated, the crystallinity affects the polarization energy values. This is in line with the observed differences in region D of our measured Xp.s. spectra of PTHF, and can probably be attributed to secondary effects consecutive to the photoionization process.

CONCLUSION

A comparison has been made between measured Xp.s. valence-band spectra of PTHF in the crystalline and amorphous states. On the basis of rather simple theoretical calculations on model molecules of limited size, differences clearly appear in the spectral region B (20–13 eV binding energy): the main difference is an intensity decrease of the antibonding structure B_5 in the spectra of amorphous PTHF. With the aid of theoretical calculations, they are interpreted as the influence of the polymer chain conformation on the electronic structure of PTHF.

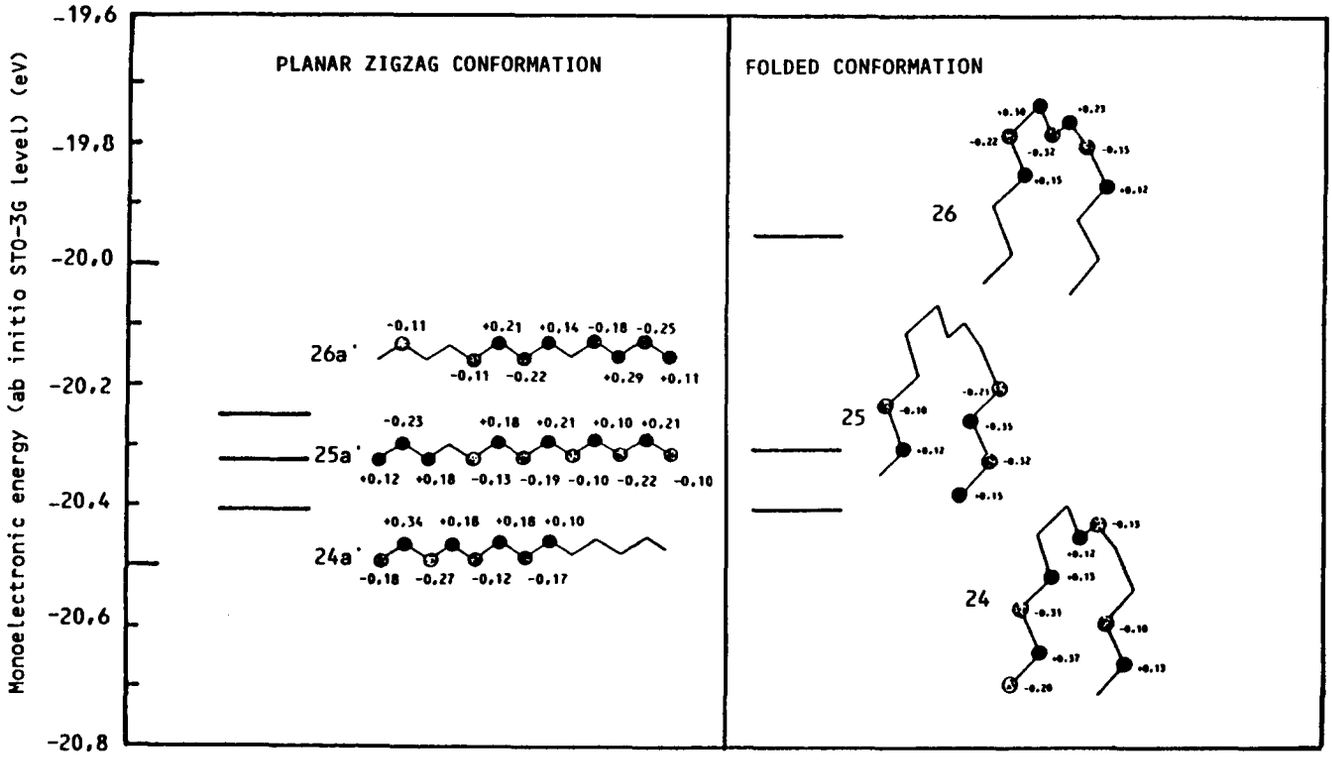

Figure 7 Schematic representation of the molecular levels generating the B_5 Xp.s. structures in the valence-band spectra of BDPBE molecule with folded and planar zigzag conformations

Table 4 Binding energy (eV) and normalized intensities (in parentheses) of peaks in the simulated and experimental Xp.s. valence-band spectra of PTHF in crystalline and amorphous states

	Crystalline				Amorphous			
Peak label	Theory[a]		Experiment		Theory[a]		Experiment	
A	33.48, 24.62	(1.00)[b]	26.3[c]	(1.00)	33.50, 24.64	(1.00)	26.5	(1.00)
B_1	27.90, 20.03	(0.79)	19.4	(0.83)	27.83, 20.00	(0.89)	19.7	(0.79)
B_2	25.06, 17.70	(0.49)	17.2	(0.77)	25.20, 17.81	(0.55)	17.2	(0.75)
B_3	23.50, 16.42	(0.38)	–	–	23.64, 16.53	(0.42)	–	–
B_4	–	–	–	–	21.88, 15.08	(0.52)	–	–
B_5	21.05, 14.40	(0.63)	14.1	(0.97)	20.90, 14.28	(0.52)	14.7	(0.88)
C_1	17.04, 11.11	(0.09)	10.8	(0.35)	16.60, 10.74	(0.13)	11.0	(0.33)
C_2	14.69, 9.18	(0.19)	8.8	–	14.94, 9.38	(0.19)	9.7	–
C_3	12.24, 7.16	(0.19)	7.4	(0.33)	12.31, 7.22	(0.22)	–	–
D_1	9.60, 4.99	(0.22)	6.1	(0.38)	9.48, 4.89	(0.23)	6.5	(0.37)
D_2	–	–	4.0	(0.18)	–	–	4.3	(0.21)

[a] *Ab initio*, contracted values; *ab initio* binding energies are contracted following the empirical relation: $E_{\text{contr.}} = 0.82E_{ab\ initio} - 2.90$
[b] Intensity normalized with respect to A peak intensity
[c] Peak binding energy values are determined by using the second derivative procedure

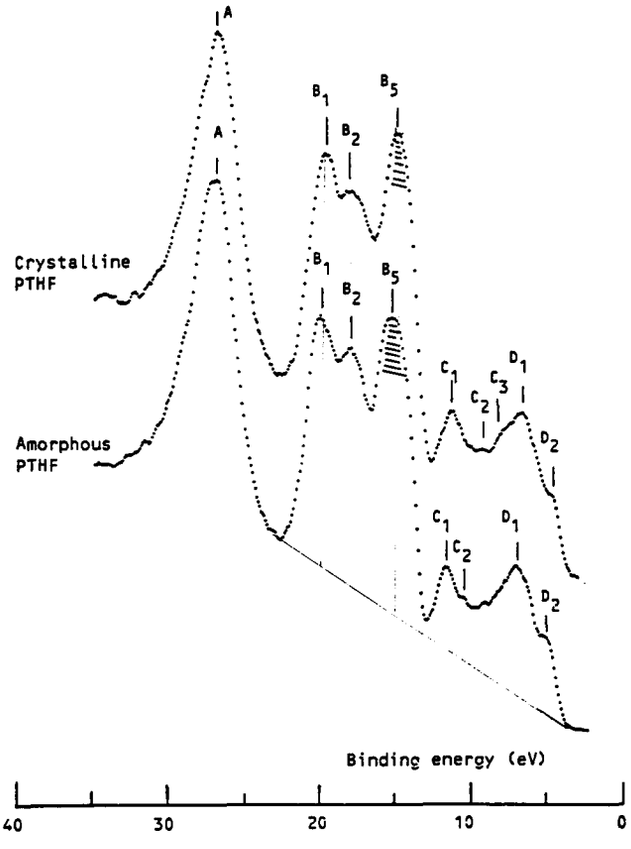

Figure 8 Experimental Xp.s. valence-band spectra of PTHF in amorphous and crystalline states

In addition, experimental spectra of polymers in both phases present some particular features in region D at lower binding energy (< 7 eV), consisting mainly of a shift of 0.3 eV of D_1 and D_2 structures towards the lower binding-energy values in the spectrum of the crystallized polymer. This may be related to a difference in the polarization energy between amorphous and crystalline polymers.

However, we have to recall that in this study, the polymer chains in the amorphous state are modelled by a folded molecule of limited size (14 atoms). So, in the future, it is obviously necessary to develop theoretical models able to perform similar theoretical calculations on larger molecules having randomly distributed folds of varying structures. It would also be most interesting to record similar spectra with the more resolved Scienta instrument and carry out variable angular analysis.

ACKNOWLEDGEMENTS

The authors acknowledge with appreciation the support of this research within the Science EEC programme no. SC1-0016-C. Computations reported in this work were carried out on the Namur Scientific Computing Facility.

REFERENCES

1 Gardella, J. A. Jr, Chen, J. S., Magill, J. H. and Hercules, D. M. *J. Am. Chem. Soc.* 1983, **105**, 4536
2 Clark, D. T. and Dilks, A. *J. Polym. Sci., Polym. Chem. Edn* 1976, **14**, 14
3 Delhalle, J. and Deleuze, M. *J. Mol. Struct. (Theochem.)* 1992, **261**, 187 and references therein
4 Delhalle, J., André, J. M., Delhalle, S., Pireaux, J. J., Caudano, R. and Verbist, J. J. *J. Chem. Phys.* 1974, **60**, 595
5 Delhalle, S., Delhalle, J., Demanet, C. and André, J. M. *Bull. Soc. Chim. Belges* 1975, **84**, 1071
6 Delhalle, J., Montigny, R., Demanet, C. and André, J. M. *Theor. Chim. Acta* 1979, **50**, 343
7 Pireaux, J. J., Riga, J., Caudano, R., Verbist, J. J. *Am. Chem. Soc. Symp. Ser.* 1981, **162**, 169
8 Delhalle, J., Delhalle, S. and Riga, J. *J. Chem. Soc. Faraday Trans. 2* 1987, **83**, 503
9 Orti, E., Brédas, J. L., Pireaux, J. J. and Ishihara, N. *J. Electron Spectrosc. Relat. Phenom.* 1990, **52**, 551
10 Deleuze, M., Denis, J. P., Dehalle, J. and Pickup, B. T. *J. Phys. Chem.* 1993, **97**, 5115
11 Delhalle, J., Riga, J., Denis, J. P., Deleuze, M. and Dosière, M. *Chem. Phys. Lett.* 1993, **210**, 21
12 Riga, J., Delhalle, J., Deleuze, M., Pireaux, J. J. and Verbist, J. J. *Surf. Interface Anal.* in press
13 Boulanger, P., Lazzaroni, R., Verbist, J. J. and Delhalle, J. *Chem. Phys. Lett.* 1986, **129**, 275
14 Boulanger, P., Riga, J., Verbist, J. J. and Delhalle, J. *Macromolecules* 1989, **22**, 173
15 Boulanger, P., Magermans, C., Verbist, J. J., Delhalle, J. and Urch, D. S. *Macromolecules* 1991, **24**, 2757
16 Boulanger, P., Riga, J., Verbist, J. J. and Delhalle, J. in 'Polymer–Solid Interfaces' (Eds J. J. Pireaux, P. Bertrand and J. L. Brédas), Institute of Physics, Bristol, 1992, pp. 315–323

17 Boulanger, P., Pireaux, J. J., Verbist, J. J. and Delhalle, J. *J. Electron Spectrosc. Relat. Phenom.* 1993, **63**, 53
18 Kretz, M., Meurer, B., Lotz, B. and Weill, G. *J. Polym. Sci. B, Polym. Phys.* 1988, **26**, 663
19 Imada, K., Myakawa, T., Chatani, Y., Tadokoro, H. and Murahashi, S. *Makromol. Chem.* 1965, **83**, 113
20 Cesari, M., Perego, G. and Mazzei, A. *Makromol. Chem.* 1965, **83**, 196
21 Hehre, W. J., Radom, L., Schleyer, P. v. R. and Pople, J. A. 'Ab Initio Molecular Orbital Theory', Wiley, New York, 1986, p. 178
22 Iguchi, M., Murase, I. and Watanabe, K. *Br. Polym. J.* 1974, **6**, 61
23 Petraccone, V., Allegra, G. and Corradini, P. *J. Polym. Sci. C* 1972, **38**, 419
24 Binkley, J. S., Frisch, M. J., De Frees, D. J., Raghavachari, K., Whiteside, R. A., Schelgel, M. B., Fluder, E. M. and Pople, J. A. Gaussian 82 program, Carnegie-Mellon University, 1982
25 Gelius, U. *J. Electron Spectrosc. Relat. Phenom.* 1974, **5**, 985
26 Koopmans, T. A. *Physica* 1933, **1**, 104
27 Sato, N., Seki, K. and Inokuchi, H. *J. Chem. Soc., Faraday Trans. 2* 1981, **77**, 1621
28 Seki, K., Tang, T. B., Mori, T., Jei, W. P., Saito, G. and Inokuchi, H. *J. Chem. Soc., Faraday Trans. 2* 1986, **82**, 1067
29 Imada, K., Tadokoro, H., Umehara, A. and Murahashi, S. *J. Chem. Phys.* 1965, **42**, 2807
30 Hümmel, D. O. 'Infrared Analysis of Polymers, Resins and Additives: Atlas, Vol. I, Plastics, Elastomers, Fibers and Resins', Wiley, New York, 1971, p. 170
31 Makino, D., Kobayashi, M. and Tadokoro, H. *Spectrochim. Acta* 1975, **31A**, 1481
32 Deleuze, M. PhD Thesis, Facultés Universitaires Notre-Dame de la Paix, Namur, Belgium, 1993